Scientific Research Report

Multiomics Data Synthesis of *FAM83H* in Amelogenesis Imperfecta

Tina Leban [a*], *Tanja Kunej* [b]

[a] *Faculty of Medicine, Department of Paediatric and Preventive Dentistry, University of Ljubljana, Ljubljana, Slovenia*
[b] *Biotechnical Faculty, Department of Animal Science, University of Ljubljana, Ljubljana, Slovenia*

ARTICLE INFO

Article history:
Received 1 September 2025
Received in revised form
24 October 2025
Accepted 1 November 2025
Available online xxx

Keywords:
Amelogenesis imperfecta
FAM83H
AI type IIIA
Enamel formation
Hypomineralization
Multi-omics

ABSTRACT

Objectives: *FAM83H* is a critical gene implicated in amelogenesis imperfecta type IIIA (AI type IIIA), but its precise role in enamel formation remains poorly understood. Fragmented datasets, inconsistent terminology, and limited integrative analyses hinder functional interpretation. This study presents a comprehensive multi-omics analysis of *FAM83H*-associated AI type IIIA.

Methods: A systematic literature search (February 2008-June 2025) was conducted in PubMed and Web of Science using targeted keywords spanning genomics, transcriptomics, epigenomics, miRNomics, proteomics, interactomics, epiproteomics, metabolomics, glycomics, lipidomics, intracellular localization, phenomics, pharmacogenomics, and environmental omics. Data were extracted using 13 bioinformatic tools and databases including Ensembl, ENCODE, OMIM, HGNC, HGMD, dbSNP, gnomAD, miRBase, TargetScanHuman, MethPrimer, dbPTM, STRING, and MalaCards.

Results: Of 150 screened publications, 62 met the inclusion criteria and were categorized across 12 omics layers. Key findings, derived from both published studies and bioinformatic databases/tools, include 38 single nucleotide polymorphisms (SNPs), two CpG islands, 932 predicted micro RNA (miRNA) binding sites, and multiple post-translational modifications. A protein–protein interaction network constructed from 18 AI-associated proteins, including FAM83H, revealed significant connectivity among enamel matrix–related proteins and provided a framework for exploring potential functional associations.

Conclusion: This study presents a multi-omics regulatory atlas of *FAM83H*, encompassing genetic variants, epigenetic changes, and post-translational modifications that are predicted to influence its biological function and role in disease.

Clinical Relevance: The integrative methodology supports *FAM83H* as a model gene for elucidating the molecular mechanisms of amelogenesis imperfecta and may facilitate improved diagnosis and targeted therapeutic strategies for AI type IIIA.

Introduction

Amelogenesis imperfecta (AI) is a heterogeneous group of inherited enamel defects that may present with or without systemic manifestations.[1] Based on clinical phenotype, AI is broadly classified into four main types: hypoplastic, hypomaturation, hypocalcified, and hypomaturation–hypoplastic with taurodontism.[1] The hypocalcified form, considered one of the most severe, typically follows an autosomal dominant inheritance pattern (amelogenesis imperfecta type IIIA, AI3A; OMIM #130900). In this type, the enamel is of normal thickness but cheesy-soft, significantly reduced in mineral content, and prone to staining. After eruption, it rapidly breaks down. On panoramic radiographs, the enamel and dentin show similar radiopacity.

Sequence variants in genes encoding secreted enamel matrix proteins (*AMELX, ENAM, AMBN*), enamel proteases

* Corresponding author. Faculty of Medicine, Department of Paediatric and Preventive Dentistry, University of Ljubljana, Vrazov trg 2, Ljubljana, 1000, Slovenia.
E-mail address: tina.leban@mf.uni-lj.si (T. Leban).
Tina Leban: http://orcid.org/0000-0002-0977-0103
Tanja Kunej: http://orcid.org/0000-0002-0465-1762
https://doi.org/10.1016/j.identj.2025.109293

(*MMP20, KLK4*), biomineralization proteins (*C4orf26*), ion transport proteins (*SLC24A4, STIM1*), cytoskeletal organization proteins (*FAM83H*, Family with Sequence Similarity 83 Member H), intracellular vesicular trafficking proteins (*WDR72*), and cellular adhesion proteins (*LAMB3, ITGB6*) have been identified as causes of non-syndromic AI, with varying inheritance patterns.[2] Variants in the *FAM83H* gene have been specifically associated with AI type IIIA,[3-5] and account for more AI cases than any other single gene.[6] The *FAM83H* gene is listed under multiple genetic database identifiers: FLJ46072 (synonym), ENSG00000180921 (Ensembl), 611927 (OMIM), 286077 (NCBI), 24797 (HGNC), and NM_198488.5 (RefSeq mRNA). It encodes the FAM83H protein (UniProt ID: Q6ZRV2; CCDS ID: CCDS6410.2). Although *FAM83H* is thought to function intracellularly in ameloblasts, its precise role in enamel formation remains unclear; it is expressed from the presecretory to secretory stages, with uncertain involvement in maturation.[7]

Recent advances in high-throughput technologies have enabled comprehensive investigations across genomics, transcriptomics, and proteomics, thereby supporting integrated approaches to the study of complex diseases. Multi-omics integration has emerged as a central theme in biomedical research,[8] providing a powerful framework for identifying previously unrecognized molecular mechanisms.[9] Despite this progress, research on *FAM83H* in the context of AI remains limited, particularly with regard to its role across multiple omic layers. Integrating genomic, epigenomic, transcriptomic, and proteomic data has proven valuable for uncovering molecular mechanisms underlying various diseases, and such an approach may also help elucidate the functional role of *FAM83H* and its involvement in AI.

This study aims to address this gap by synthesizing and integrating availeble data on *FAM83H* variants associated with AI type IIIA, organizing available genetic and molecular information across multiple omics domains, and presenting a cohesive overview to advance understanding in a broader biomedical context.

Materials and methods

Systematic literature search and data extraction

A comprehensive literature review was conducted using the PubMed and Web of Science databases, covering the period from February 2008, when *FAM83H* was first documented, through June 2025.

To ensure reproducibility, the following search strings were used. PubMed: ("amelogenesis imperfecta"[Title/Abstract] OR "AI"[Title/Abstract]) AND ("FAM83H"[Title/Abstract]) AND ("genomics" OR "transcriptomics" OR "proteomics" OR "epigenomics" OR "multi-omics"). Web of Science: Topic Search (TS) = ("amelogenesis imperfecta" OR AI) AND TS = (FAM83H) AND TS = (genomics OR transcriptomics OR proteomics OR epigenomics OR "multi-omics").

Searches were limited to English-language articles and original studies involving *FAM83H*-related AI in humans or experimental models. Reference lists of included papers were also manually screened to identify additional relevant studies.

The screening was performed independently by two authors (T.L., T.K.), with discrepancies resolved by consensus. Given the heterogeneity of study designs, no formal risk-of-bias tool was applicable.

Bioinformatic analyses

Gene annotations were verified using the Online Mendelian Inheritance in Man database (OMIM,[10] accessed May 2025, https://omim.org). Additional genomic data, including chromosomal location, synteny, sequence variants, Genomic Evolutionary Rate Profiling (GERP) scores, and Gene Ontology (GO) annotations, were retrieved from the Ensembl Genome Browser (Release 113,[11] accessed March 2025, https://www.ensembl.org), the HUGO Gene Nomenclature Committee database (HGNC,[12] accessed June 2025, https://www.genenames.org/), and the Human Gene Mutation Database (HGMD,[13] accessed June 2025, https://www.hgmd.cf.ac.uk).

Single nucleotide polymorphisms (SNPs) were obtained from the dbSNP database (Build 155,[14] accessed June 2025, https://www.ncbi.nlm.nih.gov/snp/) and referenced by their corresponding rs numbers. To complement these data and examine allele frequency information, the gnomAD database[15] (accessed June 2025, https://gnomad.broadinstitute.org/) was also consulted. In addition, constrained elements were obtained from Ensembl (Release 113 and 115, accessed October 2025, https://www.ensembl.org). These elements, defined as highly conserved genomic regions based on analyses across 92 mammalian species, were used to assess biological relevance and evolutionary conservation of the *FAM83H* gene.

MicroRNA (miRNA) annotations were retrieved from both the Ensembl database and the ENCODE Project (The ENCODE,[16] accessed May 2025, https://www.encodeproject.org). MiRNA gene symbols were aligned with miRBase v22 standards[17] (accessed May 2025, http://www.mirbase.org). MiRNA binding sites within the 3′ untranslated region (3′UTR) of *FAM83H* were identified using TargetScanHuman (Release 8.0,[18] accessed June 2025, http://www.targetscan.org).

CpG island prediction was performed using MethPrimer, applying the following criteria: CpG island length >200 bp, GC content >50.0%, and observed/expected CpG ratio >0.6[19] (accessed May 2025, http://www.urogene.org/methprimer/). The analysis encompassed a 6,000 bp upstream region, the 5′ untranslated region (5′UTR), and the first intron of *FAM83H*.

Post-translational modification (PTM) data were retrieved from the dbPTM database[20] (accessed June 2025, http://dbPTM.mbc.nctu.edu.tw/), focusing on experimentally validated modification sites. Protein–protein interaction (PPI) networks were constructed using STRING (v12.0,[21] accessed October 22nd, 2025; https://string-db.org), with all default parameters accepted and applying minimum required interaction score thresholds of 0.7 (high confidence). Depending on the level of biological relevance and informativeness, between 10 and 50 interactors were displayed. The statistical significance of network connectivity was evaluated using STRING's built-in PPI enrichment test, which determines whether the observed number of interactions is greater than

expected by chance. Networks with $p < 0.05$ were considered significantly enriched.

Genes associated with non-syndromic AI were obtained from the OMIM database and further verified using data from recent literature and the MalaCards database[22] (accessed June 2025, https://www.malacards.org).

To ensure data reliability and cross-validation across omics layers, all retrieved data were cross-referenced among multiple independent databases, including OMIM, Ensembl, HGMD, dbSNP, STRING, and dbPTM. Each variant and annotation was manually verified to confirm consistency in genomic position, transcript identity, and corresponding protein isoform. Concordance across databases and analysis layers was used as an internal validation criterion to enhance the robustness of the integrative synthesis.

Results and discussion

The integrative analysis combined data from published studies and publicly available bioinformatic databases to provide a comprehensive overview of molecular insights related to *FAM83H* in AI. The results present findings across multiple omic layers, including genomic, transcriptomic, proteomic, and epigenomic data.

Systematic literature search and and multi-omics data organization

An initial search of the PubMed and Web of Science databases identified 150 potentially relevant studies. Titles, abstracts, and full texts were reviewed to assess the availability of clinical or molecular data. Ultimately, 62 studies published between February 2008 and June 2025 met the inclusion criteria for interpretation and further analysis (Figure 1).

These studies were systematically categorized into 13 analytical perspectives, encompassing 12 distinct omics layers (Figure 2) and an additional subcellular localization analysis. Data were extracted and interpreted using 13 different bioinformatic tools and databases, which enabled the integration of multi-source molecular information across different biological domains. The omics layers include: genomics (DNA-level; 34 studies), epigenomics (including miRNomics; 2 studies), transcriptomics (11), proteomics (including interactomics; 14), epiproteomics (post-translational modifications; 2), metabolomics (including lipidomics; 2), intracellular location studies (13); phenomics (17), pharmacogenomics (2), environmental omics (1), and multi-omics (1). The studies employed either single-locus or genome-wide approaches and were conducted using both human and mouse models.

Although miRNomics is often regarded as a standalone omics layer, it is classified under epigenomics due to its gene-regulatory role without altering the DNA sequence. Similarly, interactomics was classified under proteomics due to its focus on protein–protein interactions.

Genomics-DNA level

The region on chromosome 8 (chr8: 143,723,933–143,733,801) encompassing *FAM83H* has been investigated in 34 publications reporting its implication in AI. Multiple early reports used a candidate-gene strategy, employing PCR amplification and Sanger sequencing of all exons and splice junctions of *FAM83H*.[23,3,24] In the Hart et al.[23] study, the authors also performed STRP (short tandem repeat polymorphism) genotyping for haplotype analysis. Subsequent linkage-confirming studies include Kim et al.[3] and Haubek et al.[25] Two studies used targeted NGS panels,[26,27] and more recent ones applied whole-exome sequencing (WES).

The studies reporting *FAM83H* variants associated with AI spanned a wide range of populations, including African American,[28,29] Asian,[30,28] Caucasian,[6,31-33,30,34,35,24,28] Chinese,[36,5,37-40,29,41] Chilean,[2] Colombian,[42] Danish,[25] Hispanic,[31,43,30,28] Iranian,[44] Jewish,[7] Korean,[45,3,4,46] Taiwanese,[7,35] Thai,[47-49] and Turkish[23,7] families.

Over 30 distinct *FAM83H* sequence variants associated with AI have been identified, several reported multiple times (Supplementary Table S1). All confirmed pathogenic variants are nonsense or frameshift variants producing premature stop codons between amino acids Ser^{287} and Glu^{694} within exon 5. Two missense variants have also been reported.[44,2] Because termination variants in the final exon typically escape nonsense-mediated mRNA decay (NMD),[50] the resulting truncated proteins are likely to exert a dominant gain-of-function effect, contributing to the development of AI. Of the 38 identified *FAM83H* variants, 21 have assigned reference SNP (rs) IDs in dbSNP. One variant is annotated as a Clinical Insertion (CI) and another as a Clinical Missense (CM) in the HGMD.

Evolutionary studies have also examined *FAM83H* in the context of AI. Huang et al.[51] traced its trajectory across vertebrates to clarify its role in enamel formation and how its disruption leads to AI. Based on our analysis using Ensembl, 22 constrained elements ranging from 25 to 466 bp were identified across 92 eutherian mammals, including primates (Supplementary Fig. S1). These findings indicate that *FAM83H* is conserved among species, highlighting its potential functional importance.

FAM83H is also annotated as a host gene for a miRNA. According to Ensembl and ENCODE data, *hsa-mir-4664* is located within intron 1 of *FAM83H* (Supplementary Figure S2). Intragenic miRNAs, such as *hsa-mir-4664*, may be co-transcribed with their host gene or transcribed independently via their own promoters, and can regulate downstream targets either synergistically or antagonistically relative to their host gene.[52]

The *IQANK1* gene, overlapping with the *FAM83H-203* transcript, is annotated in Ensembl and ENCODE (Supplementary Figure S2). Previously known as *FAM83H-AS1* (antisense RNA 1), it is also referred to as *ONCO-LNCRNA-3* and *CACClnc*, and is transcribed in the antisense orientation relative to *FAM83H*. Functionally, *IQANK1* has been implicated in various pathological processes. It is strongly associated with multiple cancers, including breast, colorectal, lung, prostate, and esophageal,[53-57] where it contributes to tumor progression and chemoresistance. Beyond oncology, *IQANK1* has also been linked to intervertebral disc degeneration (IVDD), where it promotes nucleus pulposus cell proliferation by sponging *hsa-miR-22-3p*, thereby supporting disc homeostasis and reducing inflammation-related pain.[58] Although no direct association between *IQANK1* and AI has been reported, its

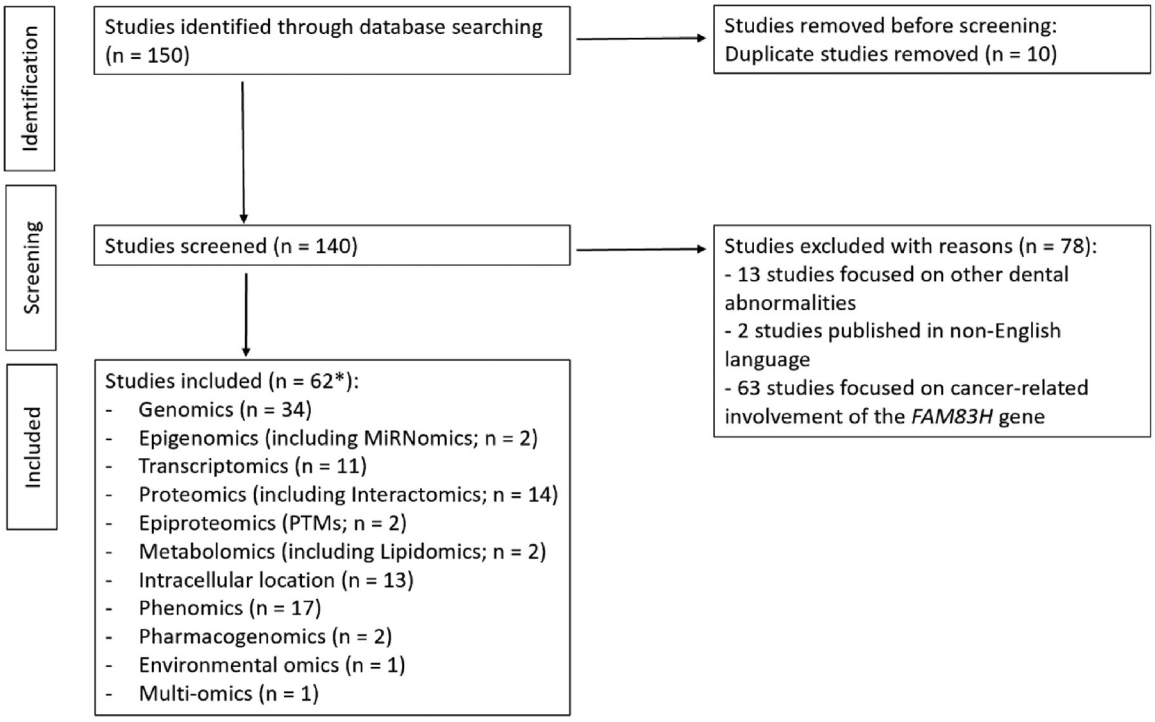

Fig. 1 – Flow diagram illustrating the study selection process. (*) Some studies contained data corresponding to multiple omics levels. Abbreviations: PTMs indicates post translational modifications.

diverse regulatory functions suggest potential relevance for further exploration in enamel-related pathways.

Epigenomics

Epigenetics refers to regulatory mechanisms such as DNA methylation, histone modifications, chromatin remodeling, and non-coding RNA (ncRNA)–mediated control, which modulate gene expression without altering the underlying DNA sequence.[59]

DNA methylation. DNA methylation, a key epigenetic modification, involves the addition of methyl groups to cytosine residues, typically at CpG dinucleotides, often resulting in

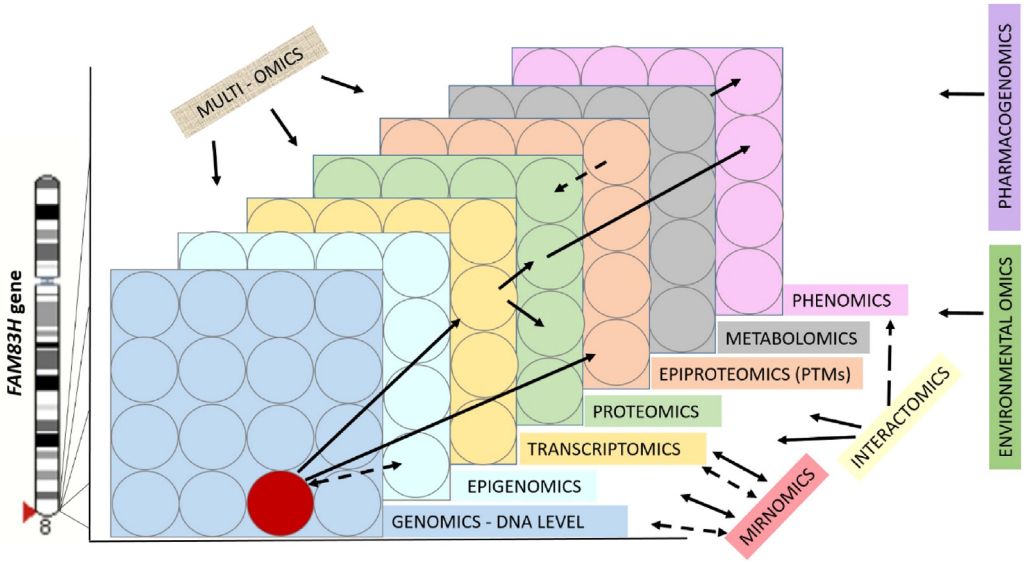

Fig. 2 – Visualization of the multiple omics levels investigated to explore the role of the *FAM83H* gene in amelogenesis imperfecta (AI). The red circle represents a genetic element (e.g., single nucleotide polymorphism - SNP, copy number variation - CNV, or insertion/deletion - indel). Arrows illustrate connections between different omics levels. For example, a SNP at the DNA level may result in the gain or loss of a CpG dinucleotide, potentially affecting methylation patterns, while post-translational modifications (PTMs) may alter protein function or stability. Solid arrows denote experimentally validated associations, while dashed arrows represent predicted/inferred relationships.

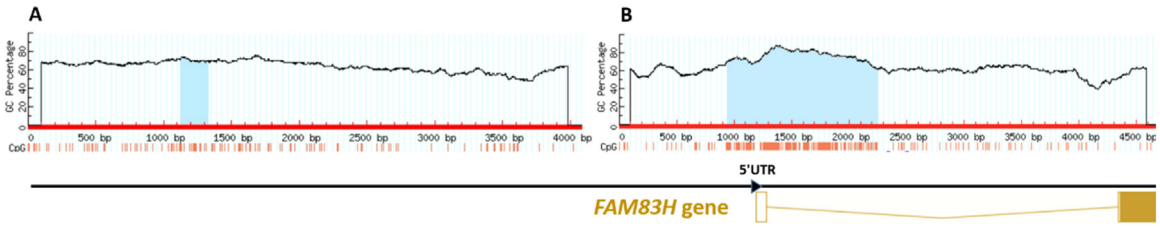

Fig. 3 – Analysis of CpG islands associated with the *FAM83H* gene using MethPrimer. (A) A smaller CpG island, 207 bp in length, located approximately 4700 to 4900 bp upstream of the gene region. (B) A larger CpG island, 1,316 bp in length, spanning the upstream region, the 5′ untranslated region (5′UTR), and the first intron of the *FAM83H* gene. To maintain consistency with the MethPrimer visualization, the *FAM83H* gene, is displayed in the forward (sense) orientation in this image; however, its actual genomic orientation is reverse (antisense).

transcriptional repression. Approximately 60–70% of human genes contain CpG islands within their promoter regions, where methylation can block transcription factor binding and suppress gene expression.[60]

While no studies have specifically examined *FAM83H* methylation in the context of AI, our MethPrimer analysis identified two CpG islands in the *FAM83H* promoter region. The smaller island is 207 bp long and located 4,700–4,900 bp upstream of the transcription start site, whereas the larger island spans 1,316 bp, covering the upstream region, 5′ untranslated region (5′UTR), and first intron (Figure 3 and Figure 4). These findings suggest regions with potential for epigenetic modification. Notably, even under stringent criteria (e.g., GC content >80%), an 834 bp island remained detectable.

Histone modifications. Histone modifications are critical for chromatin organization and gene regulation, with post-translational modifications such as methylation, acetylation, phosphorylation, ubiquitination, and sumoylation altering chromatin structure and influencing transcription.[61] For example, H3K4 methylation is typically linked to gene activation, whereas H3K9 methylation promotes gene silencing and heterochromatin formation. DNA methylation and histone modifications often act synergistically to repress transcription, frequently through recruitment of histone deacetylase complexes that condense chromatin and block transcription factor access.[62]

Beyond transcription, histone modifications are vital in development, including dental differentiation. Epigenetic silencing, via H3 trimethylation, H2A ubiquitination, and DNA methylation, regulates gene expression during odontogenesis.[63] The histone demethylase KDM6B (previously known as JMJD3) also influences dental pulp stem cell differentiation; its silencing reduces osteogenic markers and transcription factors, impairing mineralization and dentin matrix formation.[64] These findings highlight the importance of studying epigenetic regulation of *FAM83H* in enamel development and disease.

Non-coding RNA gene regulation. Non-coding RNAs can be analyzed across genomics, transcriptomics, and epigenomics, but due to their complexity and diverse regulatory roles, they are often studied as a distinct domain - ncRNA-omics. NcRNAs are broadly divided into short (<200 nucleotides) and long (>200 nucleotides) types. Among short ncRNAs, miRNAs are the most extensively studied, regulating gene expression through epigenetic and post-transcriptional mechanisms. Long non-coding RNAs (lncRNAs) include subtypes such as miRNA host genes, snoRNA host genes, lincRNAs, antisense RNAs, and intronic lncRNAs.[65] It remains unclear whether *FAM83H* interacts with any lncRNAs in AI.

MiRNAs were first implicated in tooth development by Jevnaker and Osmundsen.[66] Conditional deletion of epithelial *Dicer1* in the mouse disrupted early tooth development,[67] underscoring the role of miRNAs in enamel formation. Notably, in a murine model, *mmu-miR-153* was shown to regulate ameloblast-mediated endocytic and lysosomal pathways, and its overexpression during maturation stage of amelogenesis was associated with enamel defects resembling AI.[68,69]

MiRNAs primarily bind to the 3′ untranslated region (3′UTR) of mRNAs via their seed regions. In our study, using TargetScanHuman, we identified 932 potential miRNA binding sites within *FAM83H*, though most are poorly conserved (Figure 4).

According to miRBase, *hsa-mir-4664*, located within intron 1 of *FAM83H*, gives rise to two mature forms: *hsa-miR-4664-5p* and *-3p*. Liu et al.[70] found *hsa-miR-4664-3p* upregulated in non-small cell lung cancer (NSCLC), promoting proliferation, migration, and angiogenesis, indicating its potential as a biomarker and therapeutic target. However, no evidence currently links *hsa-mir-4664* to *FAM83H* regulation or AI.

Transcriptomics

Transcriptomics examines gene expression by analyzing differential profiles of messenger RNAs (mRNAs), and ncRNAs, such as lncRNAs, and miRNAs. Studies on *FAM83H* in AI primarily rely on animal models because they allow experimental control and genetic modification. A literature review identified 11 transcriptomic studies using systems such as cell cultures, plasmid transfection, and animal models.[36,23,3,71-74,7,38,41,75]

FAM83H is expressed in various tissues, including skin, hair follicles,[3,4,7] and has also been detected in the eyes, kidneys, liver, bladder, and larynx.[23,3,72] In addition to its role in tooth development,[73] *FAM83H* overexpression has been linked to several cancers, including colorectal,[76] hepatocellular,[77] prostate,[78] lung,[79] and gastric cancer.[80]

FAM83H expression peaks during the pre-secretory and secretory stages of ameloblasts, then declines during

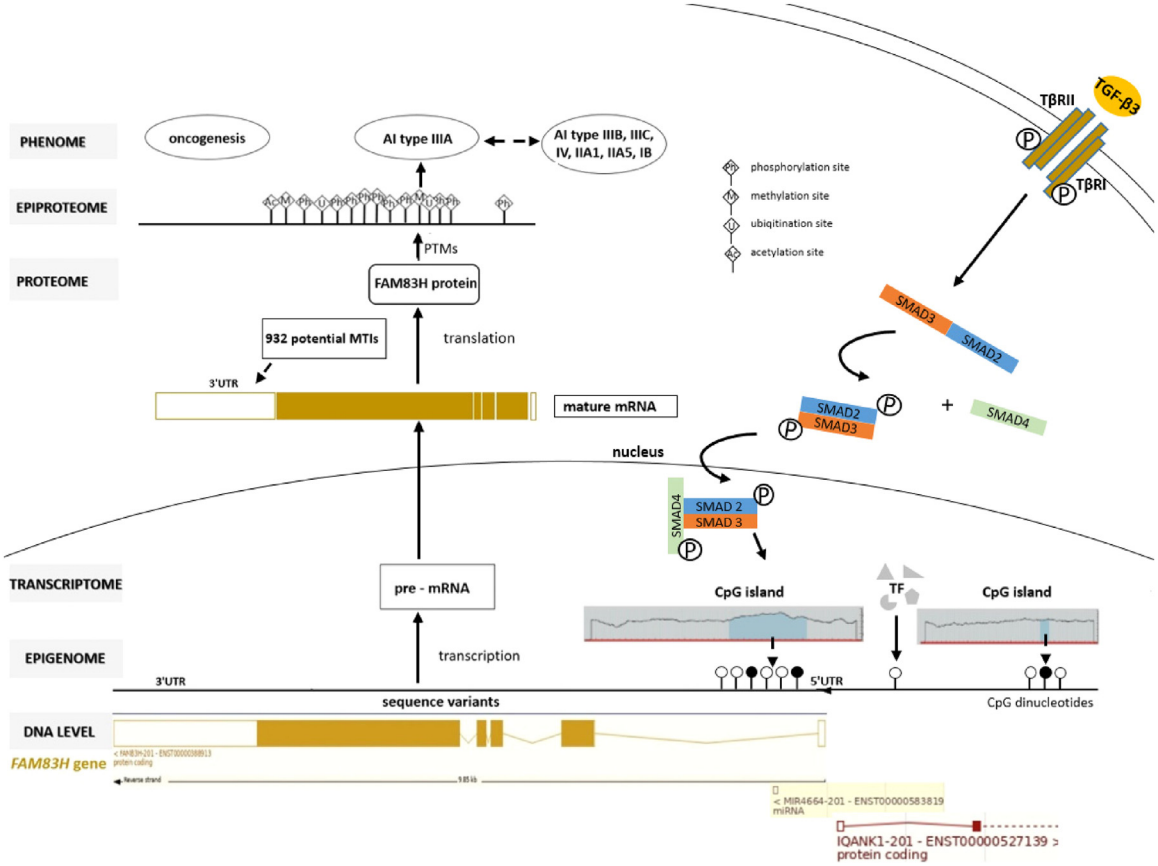

Fig. 4 – Regulatory landscape of the *FAM83H* gene based on integrated multiple omics data. The *FAM83H* transcript overlaps with two other genes: *hsa-mir-4664miRNA* and *IQANK1*, and consists of five exons, four of which are protein-coding. Exon 1 is non-coding, while exon 5, the largest, contains most of the coding sequence as well as the 3′untraslated region UTR (3′UTR). Solid black lines represent experimentally validated features, while dashed black lines indicate computational predictions. Methylated and unmethylated CpG dinucleotides are schematically shown as filled and open circles, respectively. The TGF-β3 signaling pathway involves binding to TGF-β3 to TβRII/TβRI receptors, phosphoryplation and activation of SMAD2/3, complex formation with SMAD4, nuclear translocation, and regulation of *FAM83H* gene expression. Abbreviations: PTMs – post-translational modifications; MTIs – miRNA-target interactions; TF – transcription factors; TGF-β – transforming growth factor-beta. The image is adapted from the Ensembl Genome Browser (Release 113), MethPrimer, and literature on TGF-β3 signaling (e.g.,).[74]

maturation.[3,38] Lower levels are observed in odontoblasts and alveolar bone.[73] In transgenic mice, overexpression of *Fam83h* does not affect enamel thickness or hardness,[72] and *Fam83h*-null mice show no significant reduction in hardness compared to wild-type.[7]

In vitro, altered *FAM83H* expression, via overexpression, knockdown, or truncation, disrupts keratin cytoskeleton organization.[71] Nonsense variants produce truncated mRNAs with reduced transcript levels but increased protein accumulation, likely due to impaired degradation.[36,41] In HAT-7 odontogenic epithelial cells, siRNA-mediated knockdown of *Fam83h* decreases *Enam*, *Amelx*, and *Klk4* expression, while increasing *Ambn*. Additionally, in a mouse model, transforming growth factor-beta (TGF-*β*3) signaling downregulates *Fam83h* during ameloblast maturation,[74] indicating a role in enamel gene regulation (Figure 4).

A knock-in mouse model with truncated *Fam83h* impairs enamel matrix secretion and mineralization by disrupting iron transport, *Amelx* trafficking, and cell adhesion in ameloblasts.[75] In humans, variants in *FAM83H* similarly affect enamel matrix protein secretion and ameloblast differentiation.[38] These findings highlight *FAM83H* as a key regulator of enamel protein secretion and ameloblast function, suggesting that expression variability may underlie differences in enamel development and related pathologies.

Proteomics

Proteomics examines proteins on a large scale, including their structure, function and interactions, using methods such as mass spectrometry and bioinformatics.[81] It also enables the analysis of protein-protein interactions (PPIs), post-translational modifications (PTMs), and differential protein expression.[82]

Ten studies have investigated the enamel proteins and their composition.[36,71,5,83,37,7,84,24,38,41]

The human FAM83H protein comprises 1,179 amino acids. It is encoded by five exons, with exon 5 being the largest and encoding for 933 aminoacids, which represents about 80% of

the total protein length (based on Ensembl data, Release 115). Most variants lead to truncated proteins missing the DUF1669/PACK1 domain (Ser^{287}–Glu^{694}).[24] The N-terminal domain, featuring alternating β-strands and α-helices, shares homology with the phospholipase D superfamily, forms dimers, and interacts with casein kinase I (CK1). The C-terminal domain, less structured except for some coiled regions, binds keratins.[71] Structural predictions link N-terminal variants to glycosyltransferase-like activity, and C-terminal variants to defective enamel calcification.[5] Without a signal peptide, FAM83H is likely intracellular in human ameloblasts. Studies in *Fam83h*-null mice support this, showing it is not secreted into the enamel matrix.[7]

Histological studies of hypocalcified enamel in AI type IIIA reveal altered enamel protein profiles. Wright et al.[84] observed a broad protein size range (6–200 kDa), increased tyrosine and leucine levels, but no rise in proline, compared to normal enamel. These proteins also cross-reacted with anti-amelogenin antibodies. Takagi et al.[83] identified a dominant 26 kDa amelogenin band, primarily composed of amelogenin peptides. Wright et al.[24] reported higher total protein content (1.3–5.5% vol/wt) and unique amino acid profiles enriched in serine, leucine, tyrosine, and lysine. In contrast, Wang et al.[7] found no significant differences in enamel matrix proteins, including amelogenin, among different *Fam83h* genotypes in mouse models.

Functional studies show that *FAM83H* sequence variants may elevate protein levels due to extended half-life and impaired degradation via autophagy and the proteasome.[36,41] Some variants disrupt α-helix formation, affecting protein stability, interactions, membrane assembly, and signaling, with site-specific changes producing distinct functional consequences.[37,38]

Following synthesis, the maturation and activity of both wild-type and truncated FAM83H proteins may be regulated by post-translational modifications.

Post-translational modifications (PTMs). Post-translational modifications are critical for regulating FAM83H function, stability, and interactions. Two key studies have highlighted their importance.[71,7] Wang et al.[7] identified multiple phosphorylation sites in C-terminal region of Fam83h in mice and showed that recombinant human FAM83H is phosphorylated by CK1 *in vitro*. Two conserved regions (residues 1025-1055 and 1114-1139) were proposed as functional or structural domains. The study concluded that FAM83H functions as a scaffold protein, recruiting CK1 to specific cellular sites. Truncated variants mislocalize CK1, disrupting phosphorylation and potentially contributing to disease. Similarly, Kuga et al.[71] demonstrated FAM83H's role in organizing the keratin cytoskeleton. CK1 inhibition using the small-molecule inhibitor D4476 disrupted the keratin network, altered desmoplakin phosphorylation, and reduced phosphorylation at Ser^{23} of keratin 8, suggesting FAM83H recruits CK1α to keratin filaments to regulate their structure.

In analysis using the dbPTM database, we identified multiple PTMs in FAM83H. The data indicate that FAM83H undergoes multiple phosphorylation from residue 297 onward. Additionally, 11 methylation, 8 ubiquitination, and one acetylation site (residue 1166) were identified, likely influencing its cellular functions and interactions (Figure 4).

One of the two reported missense variants in the *FAM83H* gene, c.1024T>A (p.Ser342Thr),[44] is located a known phosphorylation site (dbPTM) (Figure 5). Although both serine and threonine residues can undergo phosphorylation, this substitution may alter phosphorylation dynamics and thereby influence downstream signaling pathways.

Interactomics. Interactomics examines molecular interactions, including DNA–protein, RNA–protein, RNA–RNA interactions, to map networks governing gene expression, signaling, and regulation.[8]

Using the SPRING online algorithm,[85] Wang et al.[7] computationally predicted 89 high-confidence protein–protein interactions involving Fam83h in mice ($p < 0.05$). They proposed that FAM83H dimerizes via its N-terminal phospholipase D-like (PLD-like) domain and experimentally confirmed its interaction with CK1, mediated by a conserved F^{270}–X–X–X–F^{274}–X–X–X–F^{278} motif. This interaction was facilitated by the DUF1669 domain, which was later renamed PACK1.[86,87]

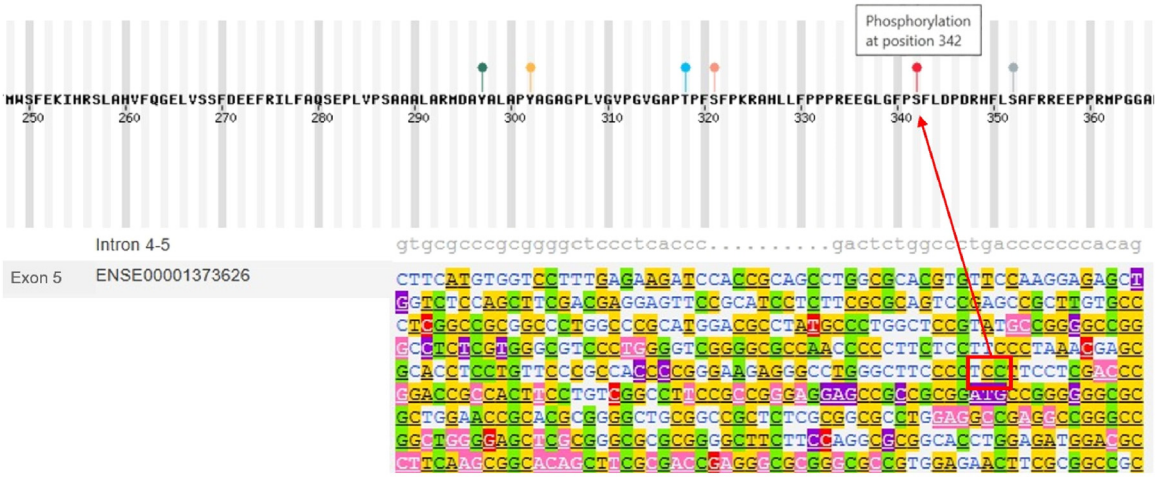

Fig. 5 – Missense variant p.Ser342Thr in *FAM83H* located at a predicted phosphorylation site. Data and figure adapted from the Ensembl Genome Browser (lower pannel) and the dbPTM database (upper pannel).

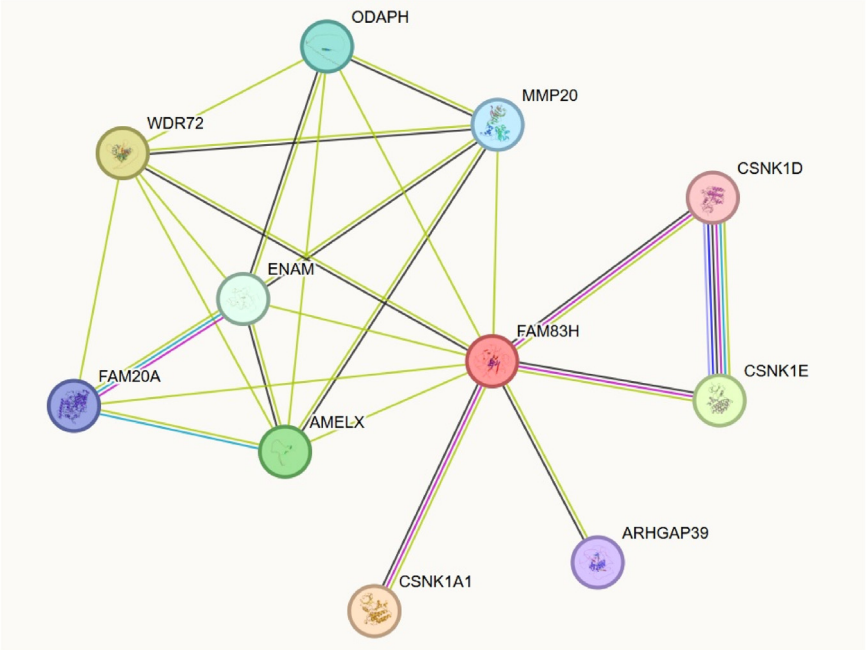

Fig. 6 – Protein–protein interaction (PPI) network associated with the FAM83H protein, generated using the STRING database. The network displays both predicted and experimentally validated interactions, including direct (physical) and indirect (functional) associations. Nodes represent proteins, and edges indicate interactions supported by curated databases, experimental evidence, or computational predictions.

In human cells, Tachie-Menson et al.[88] demonstrated interactions with NCK1/2 via C-terminal proline-rich motifs, while White et al.[89] and Kuga et al.[71] showed roles in epithelial architecture, keratin cytoskeleton organization, and desmosome formation.

We used the STRING database to explore potential PPI involving FAM83H. The analysis generated a PPI network with 11 nodes, exhibiting significantly more interactions than expected (p = 0.00014). Predicted partners include AMELX, ENAM, MMP20, FAM20A, WDR72, ODAPH, ARHGAP39, and CK1 isoforms (CSNK1A1, CSNK1D, and CSNK1E) (Figure 6).

Six proteins, AMELX, ENAM, MMP20, FAM20A, WDR72, and ODAPH, are key regulators of amelogenesis, the process responsible for enamel formation. Although not all predicted interactions have been experimentally confirmed, CK1 dysfunction has been linked to disrupted circadian rhythms,[90] aberrant Wnt signaling,[91] enamel defects due to impaired ameloblast function,[92] and genomic instability in ameloblasts,[93] all of which are critical to proper enamel development. While, ARHGAP39 regulates actin cytoskeletal dynamics via Rho GTPase signaling, influencing neuronal migration and synaptic function.[94]

Understanding these pathways not only clarifies the molecular mechanisms underlying enamel formation but also offers insights into the broader regulation of amelogenesis.

Metabolomics, glycomics and lipidomics

Metabolomics analyzes changes in small-molecule metabolites to reveal cellular processes, while specialized subfields such as glycomics and lipidomics focus on carbohydrates lipids, respectively. To date, no comprehensive metabolomic or glycomic studies specifically addressing *FAM83H* variants have been reported.

Lipidomics, a growing omics field, identifies and quantifies lipid species and their interactions with proteins, metabolites, and other lipids. Studies by Shore et al.[95] and El-Sayed et al.[43] suggest a potential role for *FAM83H* in lipid metabolism or signal transduction. Shore et al. observed abnormal lipid or lipid–protein complex retention in the enamel matrix via energy-dispersive X-ray (EDX) analysis, proposing it as a mechanism in some AI cases. Similarly, El-Sayed et al. reported elevated carbon levels in severely affected enamel, suggesting increased lipid content.

These findings offer novel insights into *FAM83H*'s role in enamel biomineralization. However, direct links between *FAM83H* and lipidomic pathways remain largely uninvestigated. Further research is needed to clarify its broader cellular functions, especially in lipid metabolism and signaling.

Intracellular location

In eukaryotic cells, mRNA is transcribed in the nucleus and translated in the cytoplasm. Since protein localization is critical to function, 13 studies have examined the intracellular distribution of FAM83H.[31,96,71,97,98,4,99,7,100,39,101,40,41]

Ding et al.[31] found Fam83h primarily in the cytoplasm of mouse ameloblasts, near the Golgi apparatus. In human, certain variants of *FAM83H* increase nuclear accumulation.[4] Wang et al.[7] suggested Fam83h/FAM83H acts as a scaffold for CK1, influencing its subcellular localization. Kuga et al.[71] confirmed FAM83H binds CK1α and localizes to perinuclear keratin filaments, extending to cell junctions.

Later studies in human cells reported that wild-type FAM83H localizes mainly to the cytoplasm, while some variants cause nuclear mislocalization.[97,39-41] This mislocalization has functional consequences, disrupting Wnt/β-catenin signaling by misdirecting CK1α, thereby blocking β-catenin nuclear entry and impairing osteogenic differentiation.[96,99,101]

These findings suggest that altered localization of FAM83H, particularly due to truncating variants, may directly drive disease pathology. In AI3A, such variants alter protein localization and exert pathogenic effects through a neomorphic rather than a loss-of-function mechanism.[4,100] The C-terminal region appears to be crucial for cytoplasmic retention, although its precise role remains unclear.[4]

Notably, not all disease-associated truncating variants result in nuclear speckle localization, indicating that mislocalization alone does not fully explain the AI3A phenotype.[98] Structurally, the DUF1669 domain enables FAM83H to access nuclear speckles and recruit CK1α, but adjacent flanking sequences are also required for complete functionality.[98] Thus, although disrupted CK1α localization and signaling likely contribute to disease pathogenesis, additional mechanisms, such as altered CK1 binding, dysregulated Wnt/β-catenin signaling, or other as yet unidentified pathways, may also be involved.[98]

Phenomics

Phenomics explores how sequence variants and environmental factors influence the phenome. To date, 17 studies have examined the phenotypic effects of *FAM83H* variants.[36,6,43,102,23,96,47,3,4,48,103,49,37,2,35,24,29]

AI type IIIA features enamel of normal thickness but impaired prism nucleation and mineralization, resulting in soft enamel that is prone to wear.[6,43,102] Two patterns are recognized: (1) a generalized form with reduced mineral content and elevated protein levels, despite near-normal prismatic structure; and (2) a localized form affecting primarily cervical enamel. Truncations yielding proteins with 677 or fewer amino acids typically cause the generalized phenotype, while those with 694 or more tend to result in localized defects.[24] Lee et al.[4] showed that the central region (Ser^{287}–Glu^{694}) is critical for normal ameloblast function, with truncations beyond this region causing nuclear mislocalization and milder phenotypes.

The first reported missense variant in *FAM83H*, reported by Urzúa et al.,[2] was associated with a milder generalized phenotype and predicted to impair disulfide bond formation, destabilizing the protein. Emerging data suggest *FAM83H* also influences dentin formation.[37,29] Nowwarote et al.[48,103] observed reduced mineralization in periodontal ligament and alveolar bone cells from mouse models carrying the p.Glu421Ter variant, indicating impaired osteogenic differentiation.

Subsequent studies expanded the phenotypic spectrum. Sriwattanapong et al.[49] reported age-dependent severity; Wang et al.[35] noted delayed eruption of canines or second molars and enamel hypoplasia. Bai et al.[36] building on Kantaputra et al.[47] showed intra-familial variability and the first evidence of incomplete penetrance in *FAM83H*-related AI.

Craniofacial abnormalities have also been reported. Kim et al.[3] and Wright et al.[24] identified increased rates of Class III malocclusion and anterior open bite. He et al.[96] found that *Fam83h*$^{Gln396Ter/Gln396Ter}$ mice exhibited reduced serum alkaline phosphatase (ALP) levels and bone calcium, suggesting impaired osteogenic differentiation, possibly via disrupted Wnt/β-catenin signaling, contributing to delayed skeletal development and reduced mandibular bone mass.

These findings illustrate the diverse and variable phenotypes associated with *FAM83H* variants, some overlapping with other disorders. To explore these links, we used MalaCards to identify diseases sharing one or more genes with AI type IIIA (AI3A) and constructed a disease network where nodes represent diseases and edges reflect shared genetic associations (Supplementary Figure S3).

This analysis revealed genetic links between AI3A and other AI subtypes. For istance, type IIIB is linked to *AMTN* variants and displays a similarly hypocalcified enamel phenotype; type IIIC, associated with *RELT* variants, causes enamel hypomineralization; and type IV (*DLX3*-related) often features taurodontism. Hypomaturation types IIA1 and IIA5, associated with *KLK4* and *SLC24A4* variants respectively, disrupt enamel maturation, while type IB (*ENAM*-related) results in localized hypoplasia. Beyond AI, AI3A shares gene-based associations with conditions like pulp degeneration, dentin erosion, and tooth erosion, suggesting overlapping molecular pathways. While MalaCards lists Köhler's disease as a genetically linked condition, current evidence does not strongly support this association, which should be interpreted cautiously.

Pharmacogenomics

Pharmacogenomics explores how genetic variation influences drug responses. In dentistry, fluoride is widely used to reduce enamel demineralization, promote remineralization, and inhibit bacterial activity. While its benefits for enamel are well known, its interaction with genetic factors during odontogenesis is a growing research focus.

Two studies have examined the impact of fluoride on *FAM83H* expression.[104,105] Jia et al. showed that fluoride downregulated *Fam83h* in mouse ameloblast-like cells by inhibiting JNK and p38 mitogen-activated protein kinase pathways, impairing mineralization. Similarly, Shi et al.[105] reported that excessive fluoride reduced *Fam83h* expression in mice, leading to enamel defects and fluorosis-like phenotypes.

These findings suggest that elevated fluoride during tooth development may contribute to enamel abnormalities by modulating *FAM83H* through gene–environment interactions.

Environmental omics

Most human traits result from complex gene–environment interactions, though the mechanisms remain incompletely understood.[106] Such interactions contribute to various developmental disorders, yet their role in enamel formation remains underexplored.[107] Environmental factors, including nutrition, exposure to toxins, and disrupted signaling, may influence phenotypic outcomes through epigenetic modifications and miRNA-mediated regulation.[108]

Nutritional deficiencies, early childhood illness, or excessive fluoride intake are linked to enamel defects but are not

directly associated with AI type IIIA. In genetically predisposed individuals, however, these factors may exacerbate enamel abnormalities through gene–environment interactions.

Winter[109] observed that hereditary AI, particularly forms with enamel opacities and taurodontism, can be misdiagnosed as environmental conditions such as fluorosis. This illustrates the challenge of distinguishing genetic from environmental causes and the need for genetic testing in uncertain cases. To date, no direct causal relationship between environmental exposures and AI type IIIA has been demonstrated.

Multi-omics

Multi-omics approaches combine data from genomics, transcriptomics, proteomics, and epigenomics to explore biological functions across molecular layers. This integration offers a holistic view of complex traits and diseases by capturing interactions between pathways.[8]

To date, no multi-omics studies have used a positional integrative framework to identify genomic regions or regulatory networks involving *FAM83H* in the context of AI. However, recent work has begun examining broader roles of the *FAM83* gene family, including links to tumorigenesis.

Snijders et al.[110] analyzed gene expression and DNA copy number variations (CNVs) across cancers and found consistent *FAM83H* upregulation, particularly in the frequently amplified 8q region. Though rooted in cancer biology, these findings highlight the gene's broader regulatory importance and support its investigation in enamel development via integrative multi-omics.

Integration of FAM83H in the interactome of non-syndromic AI candidate genes

Over 100 genes have been implicated in both syndromic and non-syndromic forms of AI, with the latter limited to isolated enamel defects.[26,111,107]

We used the STRING database to construct a PPI network based on 18 AI-associated proteins, including FAM83H (AMELX, ARHGAP6, ENAM, AMBN, MMP20, KLK4, WDR72, ODAPH, SLC24A4, GPR68, FAM20A, LAMB3, COL17A1, ACP4, ITGB6, AMTN, and DLX3). The analysis of these 18 proteins resulted in a 15-node PPI network, including FAM83H. The network displayed significantly more interactions than expected ($p < 1.0 \times 10^{-16}$) (Figure 7). In contrast, three proteins (ARHGAP6, GPR68, and SLC24A4) showed no detectable interactions, suggesting they may be less functionally integrated. FAM83H showed interactions with AMBN, DLX3, FAM20A, MMP20, ODAPH, and WDR72, indicating its integration within a highly interconnected enamel matrix cluster; however, most interactions of FAM83H were predicted based on gene neighborhood. As STRING integrates computational predictions, text mining, and available experimental data, experimental validation is required to confirm the biological relevance of the predicted associations.

Integrative multi-omics perspective

The combined evidence across omics layers suggests a multistep pathogenic cascade underlying *FAM83H*-related AI. Genomic variants, particularly nonsense or missense changes within the conserved DUF1669 domain, may not only truncate the FAM83H protein but could also potentially affect local chromatin organization. To date, all pathogenic *FAM83H* variants linked to AI have been identified within exon 5. Available data indicate that no *FAM83H* variants

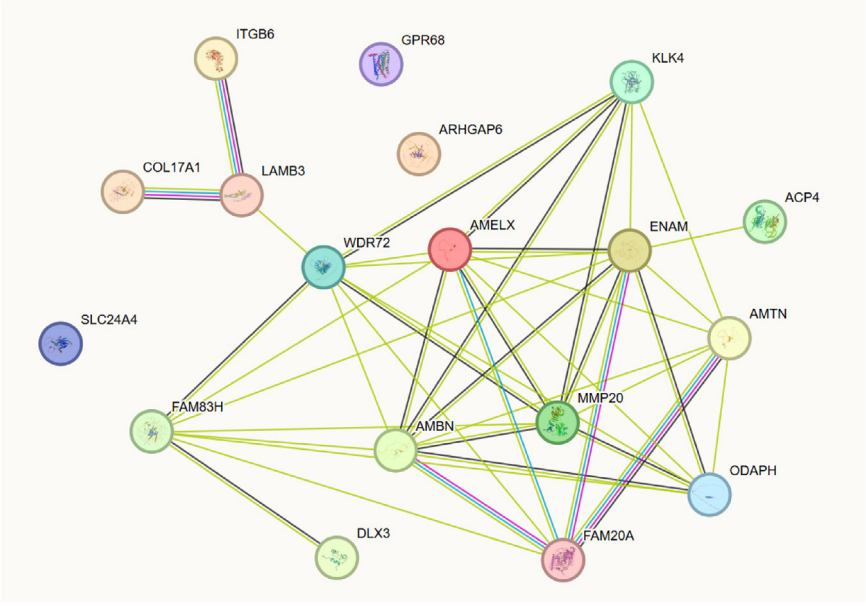

Fig. 7 – Protein–protein interaction (PPI) network constructed using the STRING database based on 18 AI-associated proteins, including FAM83H. The network shows significant interconnectivity among enamel matrix–related proteins, while three proteins (ARHGAP6, GPR68, and SLC24A4) display no detectable interactions.

linked to AI have been reported downstream of the gene; however, one missense variant occurs within a known post-translational modification site, potentially affecting protein phosphorylation, stability, and the gain and/or loss of protein −protein interactions.

At the proteomic level, our findings align with previous reports suggesting that the truncated protein may lose key phosphorylation and interaction sites, impairing binding with enamel matrix proteins such as AMELX, ENAM, and MMP20. Together, these cross-layer insights integrate previously published mechanisms with our new findings, outlining how genomic and proteomic alterations converge to produce the characteristic hypocalcified enamel phenotype observed in *FAM83H*-related AI.

This holistic approach and integrative protocol applied in this study serves as a model for single-gene analysis in rare diseases, demonstrating how systematic synthesis across omics layers can contribute to understanding potential molecular mechanisms underlying gene function and disease pathogenesis. Furthermore, this perspective highlights the potential for developing novel biomarkers to support early diagnosis and patient stratification, and provides opportunities for translational applications to guide personalized management and inform future targeted therapeutic strategies.

Limitation of the study

Although this study integrates data from multiple omics approaches, several limitations should be noted. Methodological differences, varying sample sizes, and inconsistent data processing across the referenced studies may affect comparability. Furthermore, the evidence base is largely derived from case reports or small cohort studies, warranting cautious interpretation. Most available data come from human and mouse studies, with limited experimental models to clarify the mechanistic role of *FAM83H* in enamel development. Environmental influences and gene−environment (G×E) interactions were conceptually addressed but not empirically evaluated. Certain omics layers, particularly lipidomics and glycomics, remain underexplored in relation to *FAM83H* and deserve further investigation. Finally, phenotypic variability and incomplete penetrance in *FAM83H*-associated AI underscore the need to examine potential modifier genes, epigenetic factors, and other modulators of disease expression.

Future directions

To adress current limitations, future research should priotize large-scale, multi-omics and single-cell studies supported by experimental validation to deepen understanding of *FAM83H*-associated AI. Collaboration among research groups will be essential for generating robust and diverse datasets across populations and developmental stages. Emerging technologies, such as single-cell RNA sequencing (scRNA-seq), spatial transcriptomics, and pathway mapping, offer high-resolution insights into the cellular and molecular basis of AI. Notably, no scRNA-seq studies have yet examined *FAM83H* expression or AI, whereas similar approaches have successfully revealed molecular and genetic drivers in dental caries,[112] highlighting an opportunity for future targeted single-cell transcriptomic analyses in AI. Public resources like the GTEx database[113] can also be leveraged to explore broader gene expression patterns.

Conclusions

This study proposes a comprehensive framework for mapping *FAM83H* regulation by integrating data from 13 bioinformatic databases and tools, complemented by evidence from the literature, across 12 omics layers. Unlike prior research limited to isolated factors, our multi-omics approach unifies diverse datasets into a cohesive model, offering a deeper, more interconnected view of *FAM83H*'s biological roles and clinical relevance. Its pleiotropic functions, in enamel formation, cytoskeletal organization, vesicle transport, and cancer biology, highlight its significance beyond dental pathology.

The resulting multi-omics integrative atlas identifies potential molecular drivers underlying phenotypic variability. It also serves as a model for studying rare genetic disorders and as a comparative reference for studies of gene function and enamel development across mammalian species. Future research should apply high-resolution, experimentally validated approaches that account both regulatory mechanisms and environmental influences to further elucidate *FAM83H*-associated conditions.

Funding

This work was supported by the Slovenian Research and Innovation Agency (ARIS), research program P4-0220.

Data availability

All data generated or analyzed during this study are included in this published article and its online supplementary materials. Further information and requests for materials are available from the corresponding authors upon reasonable request.

Author contributions

Tina Leban: Acquisition of data, methodology, data curation, formal analysis, writing – original draft, writing – review and editing, investigation, approval of the final version to be published. *Tanja Kunej:* Conceptualization and design, methodology, data curation, writing – review and editing, approval of the final version to be published.

Conflict of interest

The authors declared no potential conflicts of interest with respect to the study, authorship, and/or publication of this article.

Supplementary materials

Supplementary material associated with this article can be found, in the online version, at doi:10.1016/j.identj.2025.109293.

REFERENCES

1. Witkop Jr CJ. Amelogenesis imperfecta, dentinogenesis imperfecta and dentin dysplasia revisited: problems in classification. J Oral Pathol 1988;17(9-10):547–53. doi: 10.1111/j.1600-0714.1988.tb01332.x.
2. Urzúa B, Martínez C, Ortega-Pinto A, et al. Novel missense mutation of the FAM83H gene causes retention of amelogenin and a mild clinical phenotype of hypocalcified enamel. Arch Oral Biol 2015;60(9):1356–67. doi: 10.1016/j.archoralbio.2015.06.016.
3. Kim JW, Lee SK, Lee ZH, et al. FAM83H mutations in families with autosomal-dominant hypocalcified amelogenesis imperfecta. Am J Hum Genet 2008;82(2):489–94. doi: 10.1016/j.ajhg.2007.09.020.
4. Lee SK, Lee KE, Jeong TS, et al. FAM83H mutations cause ADHCAI and alter intracellular protein localization. J Dent Res 2011;90(3):377–81. doi: 10.1177/0022034510389177.
5. Song YL, Wang CN, Zhang CZ, Yang K, Bian Z. Molecular characterization of amelogenesis imperfecta in Chinese patients. Cells Tissues Organs 2012;196(3):271–9. doi: 10.1159/000334210.
6. Chan HC, Estrella NM, Milkovich RN, Kim JW, Simmer JP, Hu JC. Target gene analyses of 39 amelogenesis imperfecta kindreds. Eur J Oral Sci 2011;119(1):311–23 Suppl. doi: 10.1111/j.1600-0722.2011.00857.x.
7. Wang SK, Hu Y, Yang J, et al. Fam83h null mice support a neomorphic mechanism for human ADHCAI. Mol Genet Genomic Med 2015;4(1):46–67. doi: 10.1002/mgg3.178.
8. Pirih N, Kunej T. Toward a Taxonomy for Multi-Omics Science? Terminology Development for Whole Genome Study Approaches by Omics Technology and Hierarchy. OMICS 2017;21(1):1–16. doi: 10.1089/omi.2016.0144.
9. Hočevar K, Maver A, Kunej T, Peterlin B. Sarcoidosis Related Novel Candidate Genes Identified by Multi-Omics Integrative Analyses. OMICS 2018;22(5):322–31. doi: 10.1089/omi.2018.0027.
10. Amberger JS, Bocchini CA, Scott AF, Hamosh A. OMIM.org: leveraging knowledge across phenotype-gene relationships. Nucleic Acids Res 2019;47(D1):D1038–43. doi: 10.1093/nar/gky1151.
11. Harrison PW, Amode MR, Austine-Orimoloye O, et al. Ensembl 2024. Nucleic Acids Res 2024;52(D1):D891–9. doi: 10.1093/nar/gkad1049.
12. Seal RL, Braschi B, Gray K, et al. Genenames.org: the HGNC resources in 2023. Nucleic Acids Res 2023;51(D1):D1003–9. doi: 10.1093/nar/gkac888.
13. Stenson PD, Mort M, Ball EV, et al. The Human Gene Mutation Database (HGMD®): optimizing its use in a clinical diagnostic or research setting. Hum Genet 2020;139(10):1197–207. doi: 10.1007/s00439-020-02199-3.
14. Sherry ST, Ward MH, Kholodov M, et al. dbSNP: the NCBI database of genetic variation. Nucleic Acids Res 2001;29(1):308–11. doi: 10.1093/nar/29.1.308.
15. Chen S, Francioli LC, Goodrich JK, et al. A genomic mutational constraint map using variation in 76,156 human genomes. Nature 2024;625:92–100. doi: 10.1038/s41586-023-06045-0.
16. ENCODE Project Consortium. An integrated encyclopedia of DNA elements in the human genome. Nature 2012;489(7414):57–74. doi: 10.1038/nature11247.
17. Kozomara A, Birgaoanu M, miRBase Griffiths-Jones S. from microRNA sequences to function. Nucleic Acids Res 2019;47(D1):D155–62. doi: 10.1093/nar/gky1141.
18. McGeary SE, Lin KS, Shi CY, Pham TM, Bisaria N, Kelley GM, Bartel DP. The biochemical basis of microRNA targeting efficacy. Science 2019;366(6472):eaav1741. doi: 10.1126/science.aav1741.
19. Li LC, Dahiya R. MethPrimer: designing primers for methylation PCRs. Bioinformatics 2002;18(11):1427–31. doi: 10.1093/bioinformatics/18.11.1427.
20. Li Z, Li S, Luo M, et al. dbPTM in 2022: an updated database for exploring regulatory networks and functional associations of protein post-translational modifications. Nucleic Acids Res 2022;50(D1):D471–9. doi: 10.1093/nar/gkab1017.
21. Szklarczyk D, Gable AL, Lyon D, et al. STRING v11: protein-protein association networks with increased coverage, supporting functional discovery in genome-wide experimental datasets. Nucleic Acids Res 2019;47(D1):D607–13. doi: 10.1093/nar/gky1131.
22. Rappaport N, Twik M, Plaschkes I, et al. MalaCards: an amalgamated human disease compendium with diverse clinical and genetic annotation and structured search. Nucleic Acids Res 2017;45(D1):D877–87. doi: 10.1093/nar/gkw1012.
23. Hart PS, Becerik S, Cogulu D, et al. Novel FAM83H mutations in Turkish families with autosomal dominant hypocalcified amelogenesis imperfecta. Clin Genet 2009;75(4):401–4. doi: 10.1111/j.1399-0004.2008.01112.x.
24. Wright JT, Frazier-Bowers S, Simmons D, et al. Phenotypic variation in FAM83H-associated amelogenesis imperfecta. J Dent Res 2009;88(4):356–60. doi: 10.1177/0022034509333822.
25. Haubek D, Gjørup H, Jensen LG, et al. Limited phenotypic variation of hypocalcified amelogenesis imperfecta in a Danish five-generation family with a novel FAM83H nonsense mutation. Int J Paediatr Dent 2011;21(6):407–12. doi: 10.1111/j.1365-263X.2011.01142.x.
26. Bloch-Zupan A, Rey T, Jimenez-Armijo A, et al. Amelogenesis imperfecta: next-generation sequencing sheds light on Witkop's classification. Front Physiol 2023;14:1130175. doi: 10.3389/fphys.2023.1130175.
27. Prasad MK, Geoffroy V, Vicaire S, et al. A targeted next-generation sequencing assay for the molecular diagnosis of genetic disorders with orodental involvement. J Med Genet 2016;53(2):98–110. doi: 10.1136/jmedgenet-2015-103302.
28. Wright JT, Torain M, Long K, et al. Amelogenesis imperfecta: genotype-phenotype studies in 71 families. Cells Tissues Organs 2011;194(2-4):279–83. doi: 10.1159/000324339.
29. Zhang C, Song Y, Bian Z. Ultrastructural analysis of the teeth affected by amelogenesis imperfecta resulting from FAM83H mutations and review of the literature. Oral Surg Oral Med Oral Pathol Oral Radiol 2015;119(2):e69–76. doi: 10.1016/j.oooo.2014.09.002.
30. Lee SK, Hu JC, Bartlett JD, et al. Mutational spectrum of FAM83H: the C-terminal portion is required for tooth enamel calcification. Hum Mutat 2008;29(8):E95–9. doi: 10.1002/humu.20789.
31. Ding Y, Estrella MR, Hu YY, et al. Fam83h is associated with intracellular vesicles and ADHCAI. J Dent Res 2009;88(11):991–6. doi: 10.1177/0022034509349454.
32. Kamps R, Martens H, de Koning B, Smeets B, van Geel M. Identifying a novel causal fam83h variant for autosomal dominant amelogenesis imperfecta using exome-sequencing. Mol Genet Genomic Med 2025;13(6):e70108. doi: 10.1002/mgg3.70108.
33. Leban T, Fidler A, Trebušak Podkrajšek K, et al. Integrating Imaging and Genomics in Amelogenesis Imperfecta: A Novel

Diagnostic Approach. Genes (Basel) 2025;16(7):822. doi: 10.3390/genes16070822.
34. Wang SK, Hu Y, Simmer JP, et al. Novel KLK4 and MMP20 mutations discovered by whole-exome sequencing. J Dent Res 2013;92(3):266–71. doi: 10.1177/0022034513475626.
35. Wang SK, Zhang H, Hu CY, et al. FAM83H and Autosomal Dominant Hypocalcified Amelogenesis Imperfecta. J Dent Res 2021;100(3):293–301. doi: 10.1177/0022034520962731.
36. Bai RQ, He WB, Peng Q, et al. A novel FAM83H variant causes familial amelogenesis imperfecta with incomplete penetrance. Mol Genet Genomic Med 2022;10(4):e1902. doi: 10.1002/mgg3.1902.
37. Tan L, Guo Y, Zhong MM, et al. Tooth ultrastructure changes induced by a nonsense mutation in the FAM83H gene: insights into the diversity of amelogenesis imperfecta. Clin Oral Investig 2023;27(10):6111–23. doi: 10.1007/s00784-023-05228-3.
38. Xie Y, Meng M, Cao L, et al. Amelogenesis imperfecta in a Chinese family resulting from a FAM83H variation and the effect of FAM83H on the secretion of enamel matrix proteins. Clin Oral Investig 2023;27(3):1289–99. doi: 10.1007/s00784-022-04763-9.
39. Xin W, Wenjun W, Man Q, Yuming Z. Novel FAM83H mutations in patients with amelogenesis imperfecta. Sci Rep 2017;7(1):6075. doi: 10.1038/s41598-017-05208-0.
40. Yu S, Quan J, Wang X, et al. A novel FAM83H mutation in one Chinese family with autosomal-dominant hypocalcification amelogenesis imperfecta. Mutagenesis 2018;33(4):333–40. doi: 10.1093/mutage/gey019.
41. Zheng Y, Lu T, Chen J, et al. The gain-of-function FAM83H mutation caused hypocalcification amelogenesis imperfecta in a Chinese family. Clin Oral Investig 2021;25(5):2915–23. doi: 10.1007/s00784-020-03609-6.
42. Alvarez C, Aragón MA, Lee Y, et al. A recurrent FAM83H mutation in an extended Colombian family and variable craniofacial phenotypes. Children (Basel) 2022;9(3):362. doi: 10.3390/children9030362.
43. El-Sayed W, Shore RC, Parry DA, Inglehearn CF, Mighell AJ. Ultrastructural analyses of deciduous teeth affected by hypocalcified amelogenesis imperfecta from a family with a novel Y458X FAM83H nonsense mutation. Cells Tissues Organs 2010;191(3):235–9. doi: 10.1159/000252801.
44. Pourhashemi SJ, Ghandehari Motlagh M, Meighani G, et al. Missense Mutation in Fam83H Gene in Iranian Patients with Amelogenesis Imperfecta. Iran J Public Health 2014;43(12):1680–7 PMID: 26171361.
45. Hyun HK, Lee SK, Lee KE, et al. Identification of a novel FAM83H mutation and microhardness of an affected molar in autosomal dominant hypocalcified amelogenesis imperfecta. Int Endod J 2009;42(11):1039–43. doi: 10.1111/j.1365-2591.2009.01617.x.
46. Song JS, Lee Y, Shin TJ, Hyun HK, Kim YJ, Kim JW. Identification of a Novel FAM83H Mutation and Management of Hypocalcified Amelogenesis Imperfecta in Early Childhood. Children (Basel) 2022;9(3):429. doi: 10.3390/children9030429.
47. Kantaputra PN, Intachai W, Auychai P. All enamel is not created equal:Supports from a novel FAM83H mutation. Am J Med Genet A 2016;170A(1):273–6. doi: 10.1002/ajmg.a.37406.
48. Nowwarote N, Theerapanon T, Osathanon T, Pavasant P, Porntaveetus T, Shotelersuk V. Amelogenesis imperfecta: A novel FAM83H mutation and characteristics of periodontal ligament cells. Oral Dis 2018;24(8):1522–31. doi: 10.1111/odi.12926.
49. Sriwattanapong K, Nitayavardhana I, Theerapanon T, et al. Age-related dental phenotypes and tooth characteristics of FAM83H-associated hypocalcified amelogenesis imperfecta. Oral Dis 2022;28(3):734–44. doi: 10.1111/odi.13780.
50. Nagy E, Maquat LE. A rule for termination-codon position within intron-containing genes: when nonsense affects RNA abundance. Trends Biochem Sci 1998;23(6):198–9. doi: 10.1016/s0968-0004(98)01208-0.
51. Huang W, Yang M, Wang C, Song Y. Evolutionary analysis of FAM83H in vertebrates. PLoS One 2017;12(7):e0180360. doi: 10.1371/journal.pone.0180360.
52. Liu B, Shyr Y, Cai J, Liu Q. Interplay between miRNAs and host genes and their role in cancer. Brief Funct Genomics 2018;18(4):255–66. doi: 10.1093/bfgp/elz002.
53. Feng B, Wang G, Liang X, et al. LncRNA FAM83H-AS1 promotes oesophageal squamous cell carcinoma progression via miR-10a-5p/Girdin axis. J Cell Mol Med 2020;24(16):8962–76. doi: 10.1111/jcmm.15530.
54. Liu B, Qian D, Zhou W, Jiang H, Xiang Z, Wu D. A Novel Androgen-Induced lncRNA FAM83H-AS1 Promotes Prostate Cancer Progression via the miR-15a/CCNE2 Axis. Front Oncol 2021;10:620306. doi: 10.3389/fonc.2020.620306.
55. Lu S, Dong W, Zhao P, Liu Z. lncRNA FAM83H-AS1 is associated with the prognosis of colorectal carcinoma and promotes cell proliferation by targeting the Notch signaling pathway. Oncol Lett 2018;15(2):1861–8. doi: 10.3892/ol.2017.7520.
56. Yang F, Lv SX, Lv L, et al. Identification of lncRNA FAM83H-AS1 as a novel prognostic marker in luminal subtype breast cancer. Onco Targets Ther 2016;9:7039–45. doi: 10.2147/OTT.S110055.
57. Zhang J, Feng S, Su W, et al. Overexpression of FAM83H-AS1 indicates poor patient survival and knockdown impairs cell proliferation and invasion via MET/EGFR signaling in lung cancer. Sci Rep 2017;7:42819. doi: 10.1038/srep42819.
58. Jiang X, Chen D. LncRNA FAM83H-AS1 maintains intervertebral disc tissue homeostasis and attenuates inflammation-related pain via promoting nucleus pulposus cell growth through miR-22-3p inhibition. Ann Transl Med 2020;8(22):1518. doi: 10.21037/atm-20-7056.
59. Takahashi K, Yamanaka S. Induction of pluripotent stem cells from mouse embryonic and adult fibroblast cultures by defined factors. Cell 2006;126(4):663–76. doi: 10.1016/j.cell.2006.07.024.
60. Illingworth RS, Bird AP. CpG islands–'a rough guide'. FEBS Lett 2009;583(11):1713–20. doi: 10.1016/j.febslet.2009.04.012.
61. Venkatesh S, Workman JL. Histone exchange, chromatin structure and the regulation of transcription. Nat Rev Mol Cell Biol 2015;16(3):178–89. doi: 10.1038/nrm3941.
62. Fuks F, Hurd PJ, Wolf D, Nan X, Bird AP, Kouzarides T. The methyl-CpG-binding protein MeCP2 links DNA methylation to histone methylation. J Biol Chem 2003;278(6):4035–40. doi: 10.1074/jbc.M210256200.
63. Margueron R, Reinberg D. The Polycomb complex PRC2 and its mark in life. Nature 2011;469(7330):343–9. doi: 10.1038/nature09784.
64. Xu J, Yu B, Hong C, Wang CY. KDM6B epigenetically regulates odontogenic differentiation of dental mesenchymal stem cells. Int J Oral Sci 2013;5(4):200–5. doi: 10.1038/ijos.2013.77.
65. Chodurska B, Kunej T. Long non-coding RNAs in humans: Classification, genomic organization and function. Noncoding RNA Res 2025;11:313–27. doi: 10.1016/j.ncrna.2025.01.004.
66. Jevnaker AM, Osmundsen H. MicroRNA expression profiling of the developing murine molar tooth germ and the developing murine submandibular salivary gland. Arch Oral Biol 2008;53(7):629–45. doi: 10.1016/j.archoralbio.2008.01.014.
67. Cao H, Wang J, Li X, Florez S, Huang Z, Venugopalan SR, et al. MicroRNAs play a critical role in tooth development. J Dent Res 2010;89(8):779–84. doi: 10.1177/0022034510369304.

68. Yin K, Hacia JG, Zhong Z, Paine ML. Genome-wide analysis of miRNA and mRNA transcriptomes during amelogenesis. BMC Genomics 2014;15(1):998. doi: 10.1186/1471-2164-15-998.
69. Yin K, Lin W, Guo J, et al. MiR-153 regulates amelogenesis by targeting endocytotic and endosomal/lysosomal pathways-novel insight into the origins of enamel pathologies. Sci Rep 2017;7:44118. doi: 10.1038/srep44118.
70. Liu R, Zhang H, Xin J, et al. Novel circular RNA hsa_-circ_0036683 suppresses proliferation and migration by mediating the miR-4664-3p/CDK2AP2 axis in non-small cell lung cancer. Thorac Cancer 2024;15(27):1929–45. doi: 10.1111/1759-7714.15396.
71. Kuga T, Sasaki M, Mikami T, et al. FAM83H and casein kinase I regulate the organization of the keratin cytoskeleton and formation of desmosomes. Sci Rep 2016;6:26557. doi: 10.1038/srep26557.
72. Kweon YS, Lee KE, Ko J, Hu JC, Simmer JP, Kim JW. Effects of Fam83h overexpression on enamel and dentine formation. Arch Oral Biol 2013;58(9):1148–54. doi: 10.1016/j.archoralbio.2013.03.001.
73. Lee MJ, Lee SK, Lee KE, Kang HY, Jung HS, Kim JW. Expression patterns of the Fam83h gene during murine tooth development. Arch Oral Biol 2009;54(9):846–50. doi: 10.1016/j.archoralbio.2009.05.009.
74. Okubo M, Chiba R, Karakida T, et al. Potential function of TGF-β isoforms in maturation-stage ameloblasts. J Oral Biosci 2019;61(1):43–54. doi: 10.1016/j.job.2018.12.002.
75. Zheng X, Huang W, He Z, Li Y, Li S, Song Y. Effects of Fam83h truncation mutation on enamel developmental defects in male C57/BL6J mice. Bone 2023;166:116595. doi: 10.1016/j.bone.2022.116595.
76. Zuo L, Yang X, Lu M, et al. All-trans retinoic acid inhibits human colorectal cancer cells RKO migration via downregulating myosin light chain kinase expression through MAPK signaling pathway. Nutr Cancer 2016;68(7):1225–33. doi: 10.1080/01635581.2016.1216138.
77. Kim KM, Park SH, Bae JS, et al. FAM83H is involved in the progression of hepatocellular carcinoma and is regulated by MYC. Sci Rep 2017;7(1):3274. doi: 10.1038/s41598-017-03639-3.
78. Nalla AK, Williams TF, Collins CP, Rae DT, Trobridge GD. Lentiviral vector-mediated insertional mutagenesis screen identifies genes that influence androgen independent prostate cancer progression and predict clinical outcome. Mol Carcinog 2016;55(11):1761–71. doi: 10.1002/mc.22425.
79. Gan J, Li Y, Meng Q. Systematic analysis of expression profiles and prognostic significance for FAM83 family in non-small-cell lung cancer. Front Mol Biosci 2020;7:572406. doi: 10.3389/fmolb.2020.572406. Erratum in: Front Mol Biosci 2021; 8:653454. 10.3389 /fmolb.2021.653454.
80. Hussein UK, Ha SH, Ahmed AG, et al. FAM83H and SCRIB stabilize β-catenin and stimulate progression of gastric carcinoma. Aging (Albany NY) 2020;12(12):11812–34. doi: 10.18632/aging.103351.
81. Blackstock WP, Weir MP. Proteomics: quantitative and physical mapping of cellular proteins. Trends Biotechnol 1999;17(3):121–7. doi: 10.1016/s0167-7799(98)01245-1.
82. Pandey A, Mann M. Proteomics to study genes and genomes. Nature 2000;405(6788):837–46. doi: 10.1038/35015709.
83. Takagi Y, Fujita H, Katano H, Shimokawa H, Kuroda T. Immunochemical and biochemical characteristics of enamel proteins in hypocalcified amelogenesis imperfecta. Oral Surg Oral Med Oral Pathol Oral Radiol Endod 1998;85(4):424–30. doi: 10.1016/s1079-2104(98)90068-3.
84. Wright JT, Hall KI, Yamauche M. The enamel proteins in human amelogenesis imperfecta. Arch Oral Biol 1997;42(2):149–59. doi: 10.1016/s0003-9969(96)00096-9.
85. Guerler A, Govindarajoo B, Zhang Y. Mapping monomeric threading to protein-protein structure prediction. J Chem Inf Model 2013;53(3):717–25. doi: 10.1021/ci300579r.
86. Bozatzi P, Sapkota GP. The FAM83 family of proteins: from pseudo-PLDs to anchors for CK1 isoforms. Biochem Soc Trans 2018;46(3):761–71. doi: 10.1042/BST20160277.
87. Fulcher LJ, Bozatzi P, Tachie-Menson T, et al. The DUF1669 domain of FAM83 family proteins anchor casein kinase 1 isoforms. Sci Signal 2018;11(531):eaao2341. doi: 10.1126/scisignal.aao2341.
88. Tachie-Menson T, Gázquez-Gutiérrez A, Fulcher LJ, et al. Characterisation of the biochemical and cellular roles of native and pathogenic amelogenesis imperfecta mutants of FAM83H. Cell Signal 2020;72:109632. doi: 10.1016/j.cellsig.2020.109632.
89. White MJ, Jacobs KA, Singh T, et al. Notch1 cortical signaling regulates epithelial architecture and cell-cell adhesion. J Cell Biol 2023;222(12):e202303013. doi: 10.1083/jcb.202303013.
90. Lowrey PL, Takahashi JS. Genetics of circadian rhythms in Mammalian model organisms. Adv Genet 2011;74:175–230. doi: 10.1016/B978-0-12-387690-4.00006-4.
91. Price MA. CKI, there's more than one: casein kinase I family members in Wnt and Hedgehog signaling. Genes Dev 2006;20(4):399–410. doi: 10.1101/gad.1394306.
92. Smith CE, Nanci A. Overview of morphological changes in enamel organ cells associated with major events in amelogenesis. Int J Dev Biol 1995;39(1):153–61 PMID: 7626402.
93. Knippschild U, Gocht A, Wolff S, Huber N, Löhler J, Stöter M. The casein kinase 1 family: participation in multiple cellular processes in eukaryotes. Cell Signal 2005;17(6):675–89. doi: 10.1016/j.cellsig.2004.12.011.
94. Nowak FV. Porf-2 = Arhgap39 = vilse: a pivotal role in neurodevelopment, learning and memory. eNeuro 2018;5(5) ENEURO.0082-18.2018.. doi: 10.1523/ENEURO.0082-18.2018.
95. Shore RC, Bäckman B, Brookes SJ, Kirkham J, Wood SR, Robinson C. Inheritance pattern and elemental composition of enamel affected by hypomaturation amelogenesis imperfecta. Connect Tissue Res 2002;43(2-3):466–71. doi: 10.1080/03008200290000871.
96. He Z, Wang X, Zheng X, Yang C, He H, Song Y. Fam83h mutation causes mandible underdevelopment via CK1α-mediated Wnt/β-catenin signaling in male C57/BL6J mice. Bone 2023;172:116756. doi: 10.1016/j.bone.2023.116756.
97. Kuga T, Inoue N, Sometani K, et al. The conserved C-terminal residues of FAM83H are required for the recruitment of casein kinase 1 to the keratin cytoskeleton. Sci Rep 2022;12(1):11819. doi: 10.1038/s41598-022-16153-y.
98. Kuga T, Saraya M, Higuchi S, et al. The DUF1669 domain of FAM83H is required for its localization to nuclear speckles. Sci Rep 2025;15(1):12301. doi: 10.1038/s41598-025-96356-1.
99. Nasseri S, Parsa S, Vahabzadeh Z, et al. CRISPR/Cas9-Induced Fam83h Knock-out Leads to Impaired Wnt/β-catenin pathway and altered expression of tooth mineralization genes in mice. Iran J Biotechnol 2023;21(4):e3673. doi: 10.30498/ijb.2023.391902.3673.
100. Wang SK, Hu Y, Smith CE, et al. The Enamel Phenotype in Homozygous Fam83h Truncation Mice. Mol Genet Genomic Med 2019;7(6):e724. doi: 10.1002/mgg3.724.
101. Yang M, Huang W, Yang F, Zhang T, Wang C, Song Y. Fam83h mutation inhibits the mineralization in ameloblasts by activating Wnt/β-catenin signaling pathway. Biochem Biophys Res Commun 2018;501(1):206–11. doi: 10.1016/j.bbrc.2018.04.216.
102. Gadhia K, McDonald S, Arkutu N, Malik K. Amelogenesis imperfecta: an introduction. Br Dent J 2012;212(8):377–9. doi: 10.1038/sj.bdj.2012.314.
103. Nowwarote N, Osathanon T, Kanjana K, Theerapanon T, Porntaveetus T, Shotelersuk V. Decreased osteogenic activity

and mineralization of alveolar bone cells from a patient with amelogenesis imperfecta and FAM83H 1261G>T mutation. Genes Dis 2019;6(4):391–7. doi: 10.1016/j.gendis.2019.07.005.
104. Jia J, Yang F, Yang M, Wang C, Song Y. P38/JNK signaling pathway mediates the fluoride-induced down-regulation of Fam83h. Biochem Biophys Res Commun 2016;471(3):386–90. doi: 10.1016/j.bbrc.2016.02.027.
105. Shi G, Zhou Y, Guo J, et al. Immunohistochemical Localization of Fam83h During Fluorosis-induced Mouse Molar Development. J Histochem Cytochem 2018;66(9):663–71. doi: 10.1369/0022155418772289.
106. Manolio TA, Collins FS, Cox NJ, et al. Finding the missing heritability of complex diseases. Nature 2009;461(7265):747–53. doi: 10.1038/nature08494.
107. Wright JT. Enamel phenotypes: genetic and environmental determinants. Genes (Basel) 2023;14(3):545. doi: 10.3390/genes14030545.
108. Skinner MK. Environmental epigenomics and disease susceptibility. EMBO Rep 2011;12(7):620–2. doi: 10.1038/embor.2011.125.
109. Winter GB. Amelogenesis imperfecta with enamel opacities and taurodontism: an alternative diagnosis for 'idiopathic dental fluorosis. Br Dent J 1996;181(5):167–72. doi: 10.1038/sj.bdj.4809200.
110. Snijders AM, Lee SY, Hang B, Hao W, Bissell MJ, Mao JH. FAM83 family oncogenes are broadly involved in human cancers: an integrative multi-omics approach. Mol Oncol 2017;11(2):167–79. doi: 10.1002/1878-0261.12016.
111. Dong J, Ruan W, Duan X. Molecular-based phenotype variations in amelogenesis imperfecta. Oral Dis 2023;29:2334–65. doi: 10.1111/odi.14599.
112. Wang J, Yu Z, Xu W, Li Z, Guo C, Bian Q. Uncovering molecular and genetic drivers of dental caries Via scRNA-seq and mendelian randomisation. Int Dent J 2025;75(2):668–82. doi: 10.1016/j.identj.2024.10.005.
113. Coorens THH, Guillaumet-Adkins A, Kovner R, et al. The human and non-human primate developmental GTEx projects. Nature 2025;637(8046):557–64. doi: 10.1038/s41586-024-08244-9.